

Green and efficient recovery of valuable metals from spent lithium-ion batteries using molasses: Parametric optimization and performance evaluation.

Emenike G. Okonkwo^{a,b}, Greg Wheatley^a, Yang Liu^a, Yinghe He^{a,c,*}

^a College of Science and Engineering, James Cook University, Townsville, QLD 4811, Australia

^b Department of Metallurgical and Materials Engineering, University of Nigeria, Nsukka, Nigeria

^c Department of Chemical Engineering, Brunel University London, Uxbridge UB8 3PH, United Kingdom

ARTICLE INFO

Keywords:

Sugarcane molasses
Lithium-ion batteries
Critical metal recovery
Leaching
Methanesulfonic acid
Recycling

ABSTRACT

In this study, a green and efficient leaching system utilizing methanesulfonic acid (MSA) and sugarcane molasses is investigated, and conditions optimized using response surface methodology (RSM). Results show that molasses is capable of reducing the oxidation state thus facilitating the leaching of the transition metals and lithium. The dissolution rate of the metals in molasses-methanesulfonic acid media is observed to be fast and temperature dependent. >98% of all the metals can be dissolved under the optimized leaching condition of 2 M MSA, reductant dosage of 0.408 g (molasses)/g (cathode material) on a wet molasses (18.5% moisture) and dry cathode material basis, solid-liquid ratio of 50 g/L, 90 °C and 60 min. The proposed system provides an efficient waste-to-wealth approach that utilizes an agro-industrial by-product to recover hazardous metals present in spent LIBs.

1. Introduction

Lithium-ion batteries (LIBs) dominates global rechargeable battery market with its market estimated to be worth \$139.36 billion by 2026 and predicted to grow further (Fan et al., 2021; International Energy Agency, 2020). The LIBs have a finite lifespan and contain appreciable quantity of toxic and critical metals including lithium, cobalt, nickel, and manganese as well as graphite. The increasing adoption of LIBs leads to a high demand for critical metals and minerals, and the generation of large amount of spent batteries (Zhao et al., 2021). The demand for lithium, cobalt, nickel and graphite by 2040 is projected to be between 20 and 40 times of its current consumption (IEA, 2021). Given the localized and nonrenewable nature of these minerals, and their high concentration in the spent LIBs, recovery of these metals from the spent LIBs is considered essential for the sustainability of cleaner energy streams dependent on the use of LIBs (Church and Wuennenberg, 2019; Yang et al., 2021).

Much of the research attention has been focused on developing efficient battery recycling technologies (Fan et al., 2021; Miao et al., 2022; Okonkwo et al., 2021). Hydrometallurgical approach – a wet chemical process that involves leaching, separation and purification of

the leached metals and/or regeneration of cathode materials is the most widely adopted due to its flexibility and lower energy footprint (Okonkwo et al., 2021). Conventional hydrometallurgical approaches involve critical steps such as leaching, where lixiviants (e.g., acids, bases, deep eutectic solvents, ionic liquids among others) are used to solubilize the metals (Ku et al., 2016; Peeters et al., 2020; Zheng et al., 2022), and depending on oxidation state of the metals to be leached, reductants (e.g., sodium metabisulphite, sodium sulphite, hydrogen peroxide, glucose, sucrose, and hydrazine sulphate.) are also added to improve the solubility of transition metals such as cobalt and manganese (Chen et al., 2018; Gao et al., 2018; Vieceli et al., 2018; Yang et al., 2020). As a wet chemical process, the choice of reagents has a substantial impact on the process economics and the environment. Consequently, more attention is now given to the use of cheap and eco-friendly reagents including organic acids as lixiviants and agro-industrial wastes/by-products as reductants (Urias et al., 2020; Wu et al., 2020; Yan et al., 2021).

The performance of numerous organic compounds either as lixiviants or reductants has been compared with that of their inorganic counterparts commonly used in the industry (see Table S1). As reductants, carbohydrates such as glucose and sucrose can achieve similar

* Corresponding author at: Department of Chemical Engineering, Brunel University London, Uxbridge UB8 3PH, United Kingdom

E-mail address: yinghe.he@brunel.ac.uk (Y. He).

<https://doi.org/10.1016/j.hydromet.2023.106168>

Received 28 March 2023; Received in revised form 22 August 2023; Accepted 24 August 2023

Available online 4 September 2023

0304-386X/Crown Copyright © 2023 Published by Elsevier B.V. This is an open access article under the CC BY license (<http://creativecommons.org/licenses/by/4.0/>).

leaching efficiency improvement metric as inorganic reductants such as hydrogen peroxide, sodium metabisulphite among others (Chen et al., 2018). They are cheaper, more abundant, more thermally stable and are oxidized to organic acids that has the potential to further improve the leaching process (Ma et al., 2021; Marcq et al., 2009; Pagnanelli et al., 2014). As lixivants, the performance of sulfonic acids (e.g., amidosulfonic acid and methanesulfonic acids) have been reported to be at par with mineral acids (Ahn et al., 2019; Wang et al., 2019a). A study by Wang et al. (2019b) showed that methanesulfonic acid, owing to its high acidity ($pK_a = -1.9$), is a better lixivants than common carboxylic organic acids such as citric, succinic, formic, oxalic and malonic acids, and has a similar performance index as sulfuric acid – an attribute lacking in carboxylic organic acids commonly employed as lixivants in organic acid leaching processes (high leaching efficiency at high solid-liquid ratio) (Wang et al., 2019b). Unlike sulfuric acid, methanesulfonic acid is less toxic, readily biodegradable and non-oxidizing (Gernon et al., 1999). Despite the potential advantages, there is limited study on the performance of methanesulfonic acid as a lixiviant in the recovery of metals such as cobalt, nickel and manganese.

In striving to develop cheap and ecofriendly metal recovery processes, we report findings from the use of sugarcane molasses, an agro-industrial by-product, as a reductant and methanesulfonic acid as a lixiviant in the leaching of valuable metals from the cathode materials of spent LIBs. Sugarcane molasses is a cheap reductant consisting of sucrose, fructose and glucose whereas methanesulfonic acid is a strong organic acid with broad application in extractive metallurgy. Central composite design (CCD) – a response surface methodology (RSM)–based approach was employed to evaluate the relationship between leaching parameters, significant factor-factor interactions and optimal leaching conditions. Furthermore, the chemistry of the leaching of lithium, cobalt, manganese and nickel were evaluated by analyzing the leaching residues and formed metal salts. This work is both a proof-of-concept and a first report on the use of molasses and methanesulfonic acid combination in the leaching of mixed cathode materials from spent LIBs.

2. Materials and method

2.1. Materials

Battery packs from a range of mobile applications containing 18650 lithium-ion battery cells were obtained from BatteryWorld Townsville, Australia. Methanesulfonic acid (99%) was purchased from Sigma-Aldrich. Sugarcane cane molasses was obtained from Wilmar Sugar, Australia. The sugar profile of the sugarcane molasses is shown in Table S2.

2.2. Experimental procedure

2.2.1. Pre-treatment

Battery packs were manually dismantled, and the cells discharged in 10 wt% NaCl solution for 48 h. Discharged battery cells were washed and dried before manual dismantling to separate the battery components. Cathode materials were obtained by a sodium hydroxide-assisted delamination of the cathode current collectors, after which the recovered cathode materials were dried at 80 °C for 24 h and pulverized using a ball mill. The mean particle size of the cathode material is ~16 µm (measured using a Malvern Mastersizer 3000).

2.2.2. Reductive leaching

All leaching experiments were performed in a 250 mL round bottom flask heated and stirred with a hot plate equipped with a magnetic stirrer. For each experimental run, a 50 mL solution containing pre-determined amounts of methanesulfonic acid and sugarcane molasses were heated to a pre-determined temperature. Afterwards, a preset amount of the cathode material is added, and the mixture stirred at 400 rpm at a constant temperature throughout the duration of the leaching

process. On completion, the leaching liquor were filtered, and the residue oven dried for further analyses.

2.2.3. Experimental design and statistical analysis

Acid concentration, reductant dosage and S/L ratio are three most significant parameters affecting the leaching of metals from spent cathode materials (Cheng et al., 2019; Fan et al., 2020). Preliminary experiments, based on full factorial design, was used to explore the possible curvature and interaction effects, which are required for the optimisation of these parameters using RSM. Herein, factor ranges of 0.5–2.5 M for acid concentration, 0–1 g/g for dosage of reductant/cathode materials and 20–80 g/L for solid-liquid ratio were used. Duration of leaching and temperature were kept at 120 min and 90 °C respectively. Factors and their respective ranges were chosen based on published articles (Okonkwo et al., 2021). The factorial design table is shown in Table S3.

Based on the result of the preliminary investigation, the CCD was used to optimize the leaching process. The CCD method was chosen because of its efficiency with regard to fitting polynomial models and factor constraints of this study (Bahaloo-Horeh and Mousavi, 2017). Factor ranges were kept as per the preliminary experiment. However, due to factor constraints, factors were entered as alpha ranges and alpha ranges was adjusted to 2 (see Table S4). The optimal combination of the three independent factors needed for maximum leaching of the metals were obtained using the numerical optimization function in Design Expert and was performed after multi-factor ANOVA and fitting of the regression models. Predictions from the developed models were validated by performing additional experiments using the optimized conditions obtained from the model. All design of experiment, statistical analysis (ANOVA and regression model), optimization and surface plot were carried out using Design Expert 11 (Stat-Ease, Inc., USA). The factor layout and responses are shown in Table S5.

2.3. Analysis and characterization

The crystalline phases present in the cathode material and leach residue were characterized with X-ray diffraction (XRD, Bruker D2 Phaser). A scanning electron microscope (SEM, Hitachi SU5000) was used at a scanning voltage of 20 kV to analyze the morphology and particle size of the cathode material and residues while elemental mapping was done using Energy dispersive X-ray spectroscopy (EDS, Oxford Instruments). Changes in the functional groups due to oxidation of molasses was assessed using Fourier transform Infra-red spectroscopy (FT-IR, PerkinElmer). Scans were taken over the range of 4000 to 500 cm^{-1} using a resolution of 4 cm^{-1} . The concentration of the metals (Co, Li, Mn and Ni) in the cathode material and leaching solution were determined using an inductively coupled plasma atomic emission spectrometer (ICP-AES, Thermofisher). For the determination of the concentration of metals in the cathode material, 0.5 g of cathode material was digested in 10 mL aqua regia solution ($\text{HCl}:\text{HNO}_3 = 3:1 \text{ v/v}$) at 90 °C for 4 h. Digestion was carried out in triplicate.

Leaching efficiency of the metals was calculated using Eq. (1):

$$\text{Leaching efficiency (\%)} = \frac{C_{i,l}}{C_{i,o}} \times 100\% \quad (1)$$

where $C_{i,l}$ and $C_{i,o}$ are the concentration of metal i in mg/g in the leach liquor and the digested cathode material, respectively.

The concentration of metal (C_i) is calculated with Eq. (2),

$$C_i (\text{mg.g}^{-1}) = \frac{c(\text{mgL}^{-1}) \times V(L)}{m(\text{g})} \quad (2)$$

where C_i is the concentration of metal i ; $c(\text{mgL}^{-1})$ the metal concentration obtained from ICP-AES raw data, $V(L)$ is the volume of leaching solution, $m(\text{g})$ is the mass of cathode material used during digestion or leaching.

3. Result and discussion

3.1. Composition of the cathode materials

The elemental composition of the cathode material is shown in Table S6. Nickel is the predominant element, which indicates that a majority of the mixed spent batteries was batteries of nickel intensive cathode chemistries, e.g., NCM 523.

The XRD pattern of the raw cathode material is shown in Fig. S1 which contains well-defined and clear peaks akin to crystalline materials. The major peaks can be indexed to a hexagonal α -NaFeO₂ layered structure with R-3 m space group (JCPDS no: 74-0919), which indicates that the cathode material is likely an LiNi_{1-x-y}Co_xMn_yO₂ material (Fan et al., 2021). Carbon from the binders was not detected and are likely amorphous in nature.

The SEM and surface element mapping of the raw cathode material are shown in Fig. S1, which shows that the cathode material contains irregular shaped and agglomerated particles of different sizes, and the presence of oxygen, attributed to the oxide nature of cathode materials, and primary metals elements such as nickel, manganese and cobalt. Large quantities of carbon, most likely from the binder, and minute quantities of copper and aluminum, from current collectors, are also detected while lithium is too light an element to be detected by EDS.

3.2. Preliminary investigation of the leaching of the valuable metals

Full factorial-based preliminary leaching study using sugarcane molasses-methanesulfonic acid leaching system shows that the leaching efficiencies of lithium and the transition metals leached at a temperature of 90 °C for 2 h increased with acid concentration and exhibited significant curvature around the center point (acid concentration of 1.5 M), indicating that the optimal point is within the region of interest (See Fig. 1(a-d)). Leaching of metals is generally favored by increasing acid concentration because of the higher amount of H⁺ ions associated with increasing acid concentration (Roshanfar et al., 2019). However, as

shown in Fig. 1 (a-d), a further increase in the concentration of methanesulfonic acid to 2.5 M did not improve, or for some metals decreased, the leaching efficiency. This is consistent with previous observations of culmination of leaching efficiency of metals at a particular acid concentration (Li et al., 2013; Roshanfar et al., 2019). Some researchers suggested that high concentration of H⁺ can lead to rapid formation of a product layer at the initial stage, which can limit diffusion rate and consequently, cause a decrease in the overall leaching efficiency (Faraji et al., 2020; Li et al., 2022).

Fig. 1 (a-d) also show that the leaching efficiency of all the metals (Co, Li, Mn and Ni) were enhanced as the reductant dosage increased from 0 to 0.5 g/g and declined afterwards. The decrease in leaching efficiency was more severe for lithium, which fell below the average value as the reductant dosage increased to 1 g/g. This is likely due to unwanted side reactions between components of molasses and methanesulfonic acid that is more probable at high reductant dosage; this reaction can also reduce the amount of acid available for leaching of the metals.

A reduction in efficiency was also observed above an S/L ratio of 50 g/L. This is consistent with previous reports and can be attributed to the fact that high S/L ratio increases the viscosity of the solution, hampers diffusion of species and affects the concentration distribution of the lixiviant (Faraji et al., 2020).

3.3. Leaching of lithium and transition metals based on RSM design

3.3.1. Statistical analysis and model establishment

Based on the result of the preliminary investigation using factorial design which showed that curvature is significant, CCD was used for the optimization of the leaching parameters. The results from CCD design presented in Table S5 in which acid concentration, dosage of reductant and S/L ratio were set at five levels shows that the leaching efficiencies of cobalt, lithium, manganese and nickel ranges from (26.1 to 99.9%, 47.6 to 99.9%, 27.0 to 99.9% and 26.0 to 99.9%, respectively. Complete dissolution can be achieved at acid concentration of 1.5 M, reductant dosage of 0.5 g/g and S/L ratio of 20 g/L.

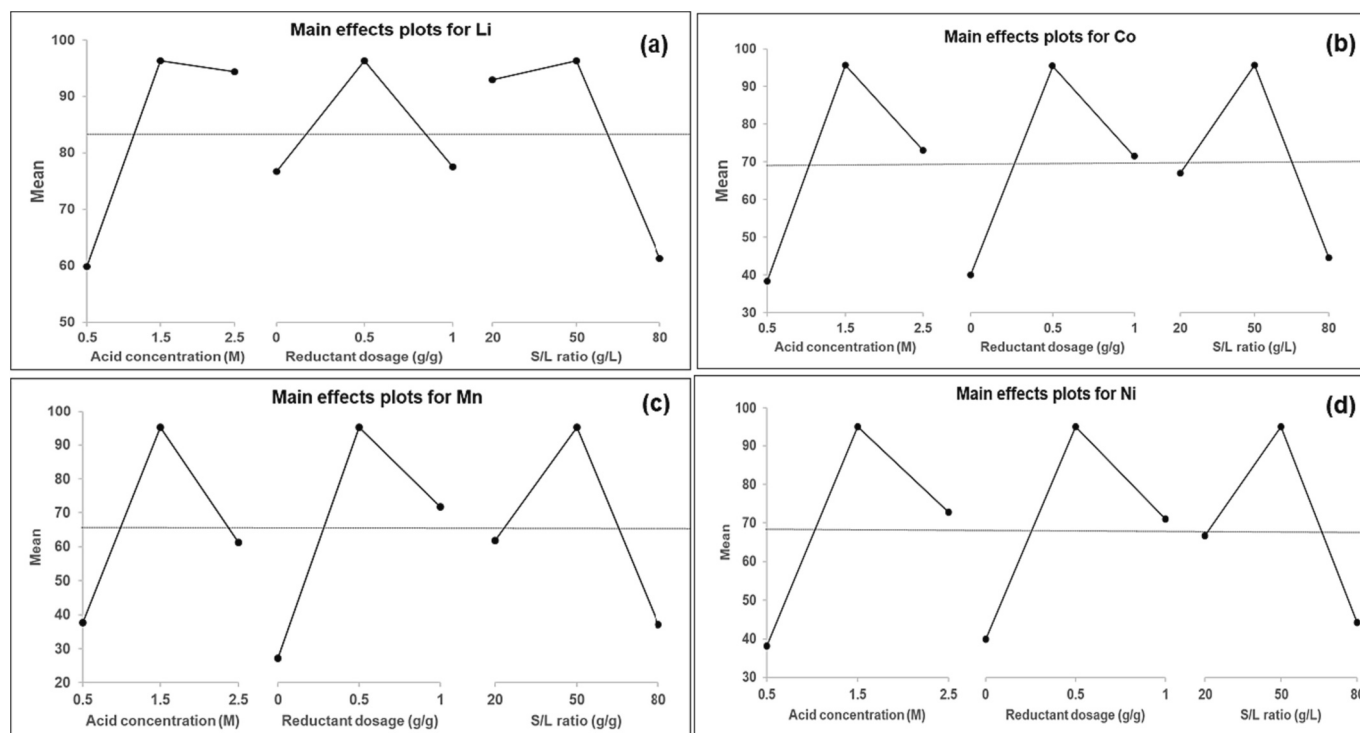


Fig. 1. Main effects plot for (a) Lithium (b) Cobalt (c) Manganese and (d) Nickel (leaching temperature and time kept at at 90 °C and 120 min).

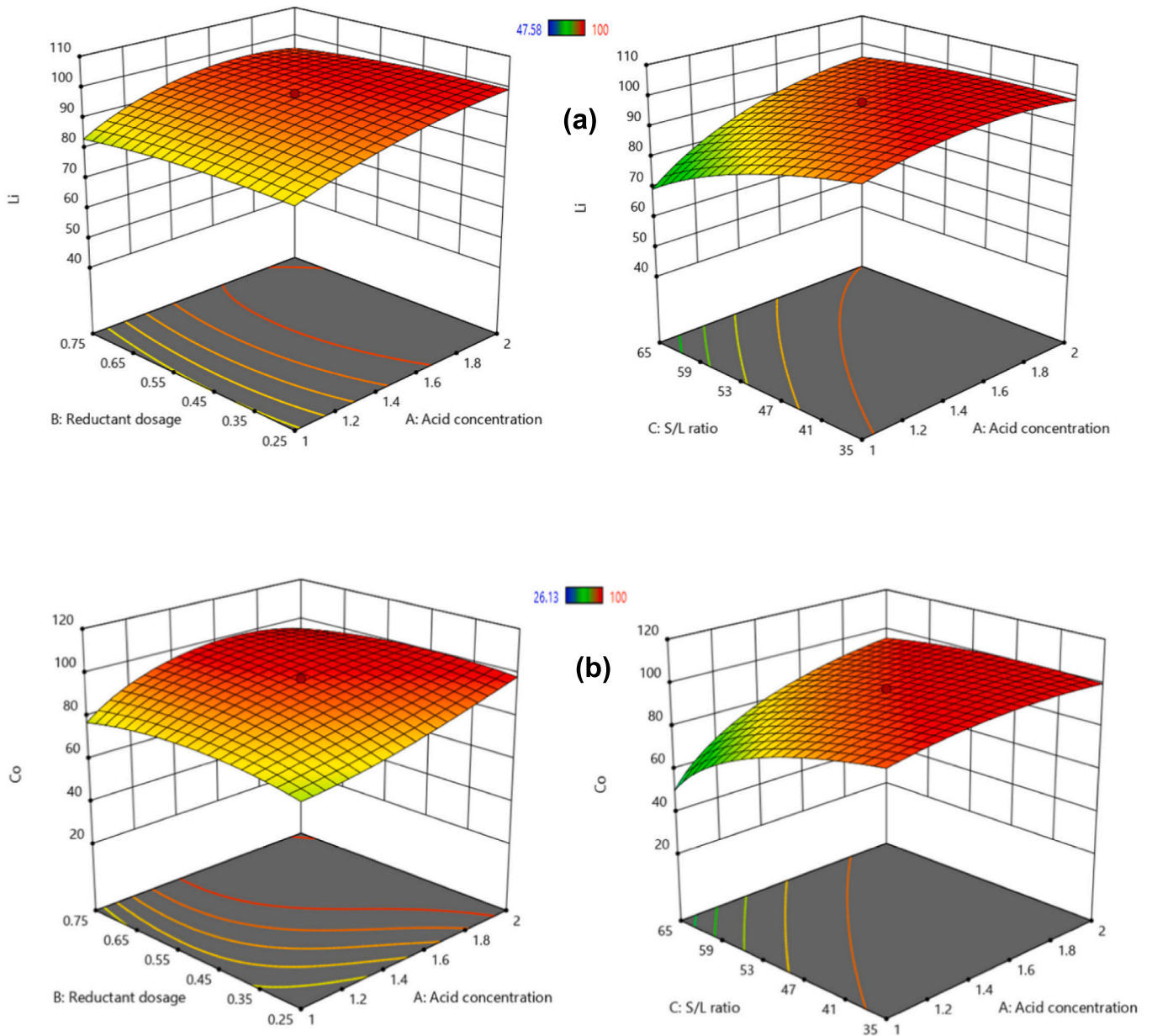


Fig. 2. RSM plots for (a) Li (b) Co (c) Mn and (d) Ni (leaching temperature and time kept at 90 °C and 120 min).

Regression analysis of the experimental data after Box-Cox transformation ($\lambda = 3$) showed that reduced cubic model can be used to correlate the leaching parameters to the observed leaching efficiencies (See supplementary data for details of the model development). Eqs. (3)–(6) show the generalized prediction model in coded units of the metals. The equations contain only significant terms and terms needed for model hierarchy.

$$\begin{aligned}
 (LE_{Li})^3 &= 9.019 \times 10^5 + 1.627 \times 10^5 A + 10767.37B - 1.490 \times 10^5 \\
 &\quad C - 16448.55AB + 1.016 \times 10^5 AC - 1.046 \times 10^5 A^2 - 31879.65B^2 \\
 &\quad - 44911.26C^2 - 49452.89A^2B
 \end{aligned} \tag{3}$$

$$\begin{aligned}
 (LE_{Co})^3 &= 8.905 \times 10^5 + 2.261 \times 10^5 A + 1.770 \times 10^5 B - 2.063 \times 10^5 \\
 &\quad C - 27407.32AB + 1.0444 \times 10^5 AC - 1.033 \times 10^5 A^2 \\
 &\quad - 1.038 \times 10^5 B^2 - 74901.15C^2 - 1.951 \times 10^5 A^2B
 \end{aligned} \tag{4}$$

$$\begin{aligned}
 (LE_{Mn})^3 &= 8.803 \times 10^5 + 2.214 \times 10^5 A + 1.874 \times 10^5 B - 2.026 \times 10^5 \\
 &\quad C - 24726.88AB + 1.419 \times 10^5 AC - 99512.30A^2 \\
 &\quad - 1.070 \times 10^5 B^2 - 69139.34C^2 - 2.06 \times 10^5 A^2B
 \end{aligned} \tag{5}$$

$$\begin{aligned}
 (LE_{Ni})^3 &= 8.670 \times 10^5 + 2.188 \times 10^5 A + 1.727 \times 10^5 B - 2.04 \times 10^5 \\
 &\quad C - 24833.54AB + 1.394 \times 10^5 AC - 1.016 \times 10^5 A^2 \\
 &\quad - 1.016 \times 10^5 B^2 - 70903.66C^2 - 1.873 \times 10^5 A^2B
 \end{aligned} \tag{6}$$

where the term LE_{Me} (Me = Li, Co, Mn, Ni) is the predicted leaching efficiency for the metals. A, B and C are coded values of acid concentration, dosage of reductant and S/L ratio respectively (leaching time and temperature were kept at 120 min and 90 °C, respectively).

The actual and coded values are related by:

$$\text{Coded value} = \frac{2^*(\text{Actual factor setting} - \text{Mean of factor setting})}{\text{Factor range}} \tag{7}$$

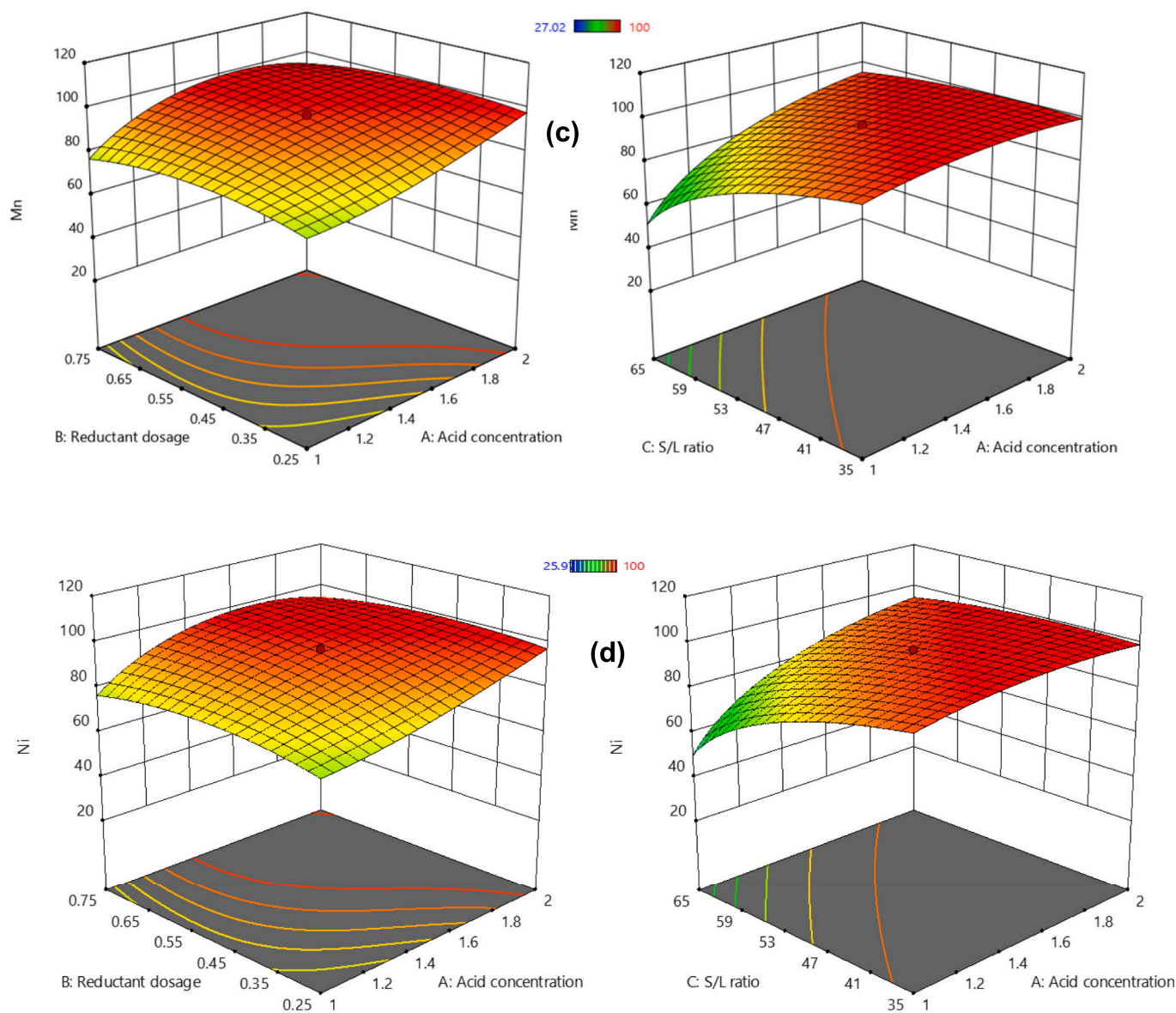


Fig. 2. (continued).

The coefficient of the coded factors from regression models is a good measure of the influence of a factor (Bahaloo-Horeh and Mousavi, 2017; Montgomery, 2017). As shown in Eqs. (3)–(6), acid concentration has the highest effect on the leaching efficiency of the metals. Its effect is higher in the leaching of the transition metals than that in lithium. The developed models also show that acid concentration and dosage of reductant had positive effect on the leaching of the metals whereas S/L ratio had a negative effect. These effects are better illustrated by the perturbation graphs shown in Fig. S2(a–d). For lithium, dosage of reductant follows a flat line unlike acid concentration and S/L ratio. This is because, owing to lithium having only one oxidation state, its leaching should theoretically not be influenced by the presence of a reductant. The change in the slope of the perturbation graphs of acid concentration and S/L ratio is because of the dependence of leaching of lithium on the available H^+ and molar ratio of the lixiviant to the cathode material (Chen et al., 2018).

The perturbation plot of the transition metals (Co, Ni and Mn) (Fig. S2b–d) revealed a steep line for S/L ratio and curved lines for acid concentration and dosage of reductant, indicating that the leaching of the transition metals is sensitive to all three factors. Steep lines reveal a

strong contrast between the low and high factor levels whereas curved lines prove the existence of curvature, which are in agreement with previous observations in section 3.2. Hence it can be deduced that reducing the S/L ratio and increasing both acid concentration and dosage of the reductant will improve the dissolution of these metals.

The model equations also illustrate that the interaction between acid concentration and dosage of reductant is negative unlike that between acid concentration and S/L ratio. This may be attributed to degradation reactions involving the carbohydrates present in molasses. Nonetheless, the coefficient of the interaction term is small relative to the main effects hence can be ignored.

The ANOVA results calculated using a significance threshold ($p < 0.05$) indicating a 95% confidence level is presented in Table S7. The results confirm that the models for all the metals are significant at a 95% confidence level with p -values of <0.0001 . The lack of fits are not significant, confirming the fitness of the model (Bahaloo-Horeh and Mousavi, 2017). The high adequate precision shown by the models suggests that the models can be used to navigate the design space (Montgomery, 2017). The significance analyses of the linear, quadratic and interaction terms are shown in Table S8–S11. For lithium, the

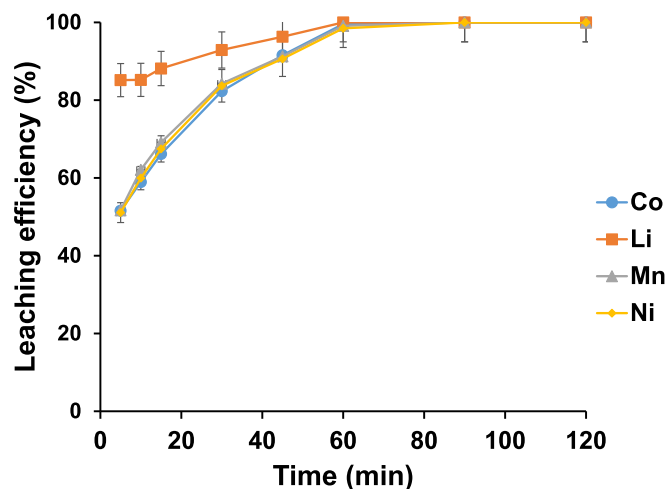


Fig. 3. Effect of leaching time on leaching efficiency at 2 M Methanesulfonic acid, 0.408 g/g reductant dosage, S/L ratio of 50 g/L, and temperature of 90 °C.

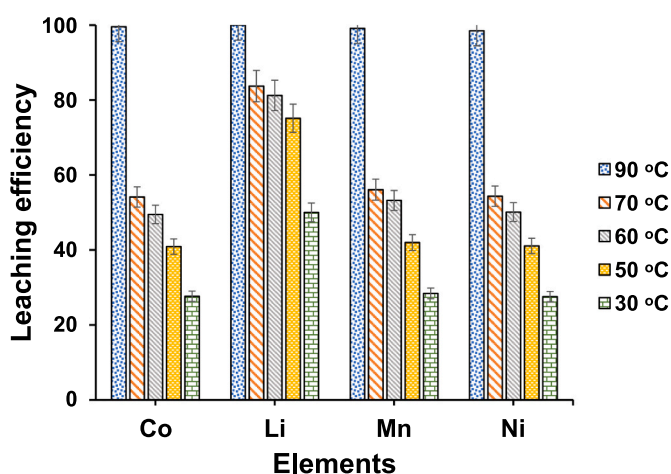


Fig. 4. Effect of temperature on leaching efficiency at 2 M Methanesulfonic acid, 0.408 g/g reductant dosage, S/L ratio of 50 g/L, and time 60 mins.

significant terms are linear terms such as acid concentration and S/L ratio ($p = 0.0001$), interaction between acid concentration and S/L ratio ($p = 0.0001$), all quadratic terms and cubic term of the interaction between the quadratic term of acid concentration and linear term of reductant dosage (See Table S8). The leaching of lithium was not significantly affected by dosage of reductant and the interaction between acid concentration and reductant dosage. This observation is not surprising because as an alkali metal, the leaching of lithium is solely dependent on the available hydrogen ions present in the leaching solution. A positive interaction exists between acid concentration and S/L ratio indicating that increasing both are beneficial to the leaching of lithium. For the transition metals, all linear terms, quadratic terms, the interaction between acid concentration and S/L ratio, and interaction between the quadratic term of acid concentration and linear term of reductant dosage are significant. Unlike lithium, part of the transition metals exist in high oxidation state hence need to be reduced to be effectively leached (Meng et al., 2020). The significant effect of reductant dosage confirms that molasses is an effective reducing agent for the leaching of all transition metals in the treated spent LIBs, namely, manganese, nickel and cobalt oxides.

The graphs of the values predicted by the model plotted against the actual experimental values are shown in Fig. S3. Both the predicted values and actual response falls close to the diagonal line indicating

strong correlation. This shows that the model is suitable for prediction and affirms the high coefficients of determination (R^2) exhibited by the fitted polynomial model.

3.3.2. Response surface plots of the leaching efficiencies of the metals

Surface plots of leaching efficiencies of lithium, cobalt, manganese and nickel against significant model terms is shown in Fig. 2 (a-d). The surface for the leaching of lithium is different from those of the transition metals, implying a different leaching rate. The leaching efficiency of lithium increased from 72.1 to 92.4% as the acid concentration increased from 1 M to 2 M. However, an increase in reductant dosage from 0.25 to 0.75 g/g did not significantly improve the leaching of lithium (94.1% versus 94.9% at acid concentration of 1 M, S/L ratio = 35 g/L). Conversely, a significant drop in the leaching efficiency can be observed as the S/L ratio increased. The drop is more predominant at low acid concentration but hardly noticeable at higher acid concentration (2 M). This suggests that the availability of hydrogen ions is the determining factor in the leaching of lithium. While previous works utilizing organic acids have shown that a high S/L ratio (>30 g/L) hampers the leaching of lithium due to decreased rate of diffusion of ions or increased viscosity (Fan et al., 2020; Faraji et al., 2020; Fu et al., 2019b; Li et al., 2017), it is evident from this work that methanesulfonic acid of 2 M concentration can be effectively used to leach lithium at S/L ratio in the range of 35–65 g/L without a significant reduction in efficiency.

The transition metals showed similar leaching behaviors as shown by the shapes of the curves (Fig. 2b-d). The leaching efficiency of these metals increased with acid concentration, consistent with trends reported in literature (Gao et al., 2018; Wang et al., 2019b). It is evident that irrespective of acid concentration (1–2 M), reductant dosage as low as 0.25 g/g can effectively achieve above 90% leaching of the metals (S/L ratio, 35–65 g/L), thus showcasing the potency of molasses as a reducing agent. Nonetheless, a slight reduction in leaching efficiency (shown by green colored areas) can be observed at higher reductant dosage (0.75 g/g). This is more predominant at lower acid concentration, which implies a competition for protons by the yet-to-be leached metals and unhydrolyzed sugars in the molasses. However, further studies on the reaction mechanisms including reaction pathways for components in molasses in an acidic environment are needed to ascertain this conjecture and will be the subject of our future study.

3.3.3. Optimization and validation of leaching conditions

A leaching efficiency of 99.9% for all the metals was achieved at an acid concentration of 1.5 M, reductant dosage of 0.5 g/g and S/L ratio of 20 g/L, as shown in Table S5. A similar leaching efficiency (>98%) for all the metals can also be obtained by slightly increasing the acid concentration to 2 M, S/L ratio to 35 g/L and reducing the reductant dosage S/L ratio to 0.25 g/g. A desirable leaching efficiency that is >95% for all the metals can also be achieved by keeping the leaching parameters at the center points (acid concentration of 1.5 M, reductant dosage of 0.5 g/g and S/L ratio of 50 g/L) (see Table S5). Economically, a high S/L ratio is preferred because it translate to a higher treatment capacity. In the model optimization, S/L ratio was kept at 50 g/L.

With the objective of maximizing the leaching of the metals at S/L ratio of 50 g/L, and acid concentration and reductant dosage at the factor range used in the RSM, the numerical optimization tool was used to obtain the optimal experimental conditions needed to achieve the intended objective. The optimal solution was selected based on calculated desirability, which reaches a value of 1 as the response nears the target values. As shown in Fig. S4, complete leaching of the metals with a desirability of 0.991 can be achieved at an acid concentration of 2 M, reductant dosage of 0.408 g/g and S/L ratio of 50 g/L.

The maximum and minimum leaching efficiencies at the optimized conditions predicted by the model at a 95% confidence interval and mean value of verification runs repeated thrice is shown in Table S12. As shown, the obtained results are within the range predicted by the model

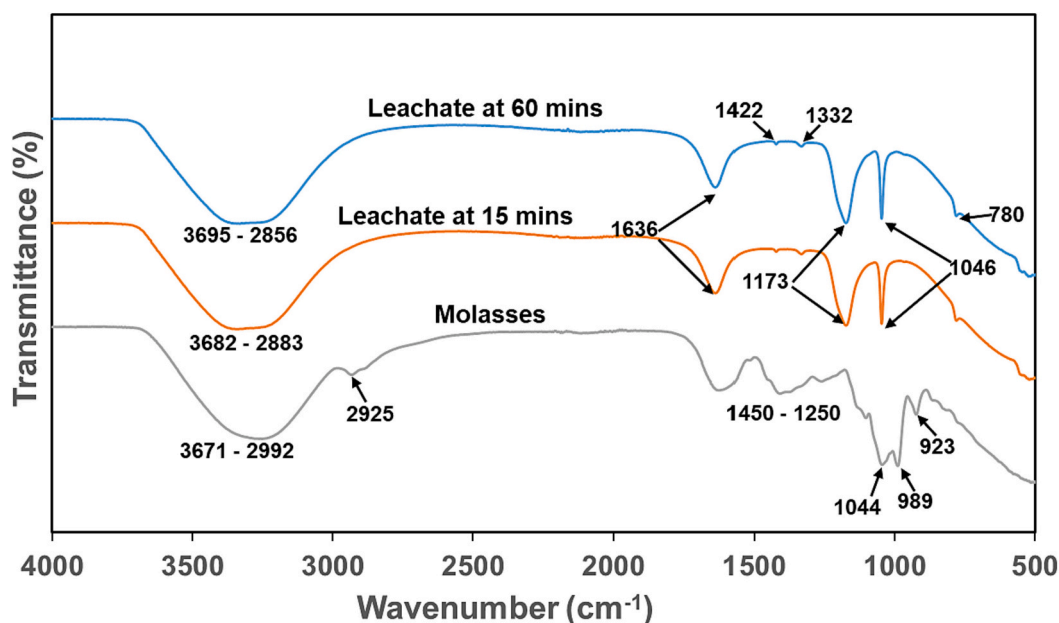


Fig. 5. FT-IR of Molasses and molasses-methanesulfonic acid leachates.

Table 1

Observed peaks and assigned groups in FT-IR spectra of molasses and leachates.

| Peak position (cm ⁻¹) | Functional group and type of vibration | Ref. |
|-----------------------------------|--|---|
| 3650–3000 | O–H stretching vibrations. | (El Darra et al., 2017; Kozłowicz et al., 2020) |
| 2925 | C–H stretching vibration of a CH ₃ group | (El Darra et al., 2017) |
| 2878 | | |
| 1636 | Deformation vibration of –OH groups in carboxylic acid | (Kozłowicz et al., 2020) |
| 1422 | CH ₃ asymmetric bend of metal methanesulfonates. | (Parker and Zhong, 2018; Zhong and Parker, 2018). |
| 1332 | | |
| 1046 | SO ₃ symmetric bend of metal methanesulfonates. | (Parker and Zhong, 2018; Zhong and Parker, 2018). |
| 1044 | C–O stretching in C–OH groups and C–C stretching of carbohydrates. | Anjos et al., 2015 |
| 1173 | C–O in the C–OH group and stretching of C–C in the sugars. | Cengiz and Durak, 2019) |
| 989 | | |
| 923 | C–H bending and C–OH stretching in sucrose and fructose. | (Anjos et al., 2015; Cengiz and Durak, 2019) |
| 780 | C–S stretching and SO ₃ asymmetric bend of metal methanesulfonates. | (Parker and Zhong, 2018) |

hence validating the adequacy of the model. The obtained leaching efficiencies are also comparable to those reported in similar studies shown in Table S1.

3.4. Influence of other leaching parameters

3.4.1. Effect of leaching time

In general, the rate of dissolution of metals increases with time till the reactants are expended or equilibrium is achieved. Hence, given enough time, optimal dissolution of all the metals will be achieved. However, leaching of metals can be fast and optimal time may be less than the time assumed, which leads to additional overall process cost due to extended leaching time. Fig. 3 shows the rate of dissolution of the metals under the optimized condition as a function of time. The extent of leaching of all metals (Co, Ni, Mn and Li) increased with time. Additionally, the leaching using molasses-methanesulfonic acid leaching system is fast, with >50% of all the metals leached out in fifteen minutes. Further, >98% of all the metals can be leached within 60 min while 99.9% efficiency can be achieved if the time is extended to 90 min. From an economic point of view, a leaching time of 60 min is sufficient and will be adopted as the new optimal leaching time.

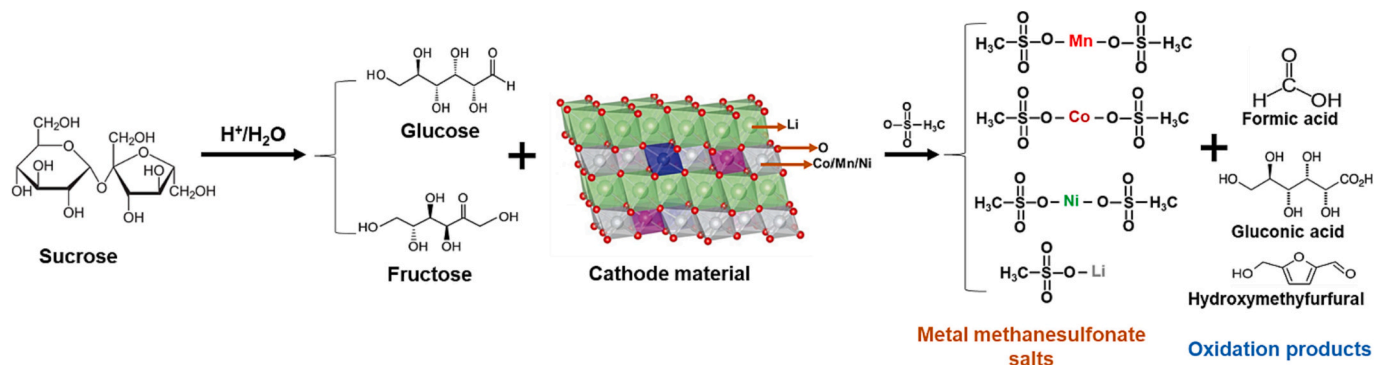


Fig. 6. Tentative reactions occurring during the leaching of transition metals in Molasses-methanesulfonic acid media.

3.4.2. Effect of leaching temperature

Leaching performance under the optimized conditions but at varied temperatures was also assessed. Intrinsically, the leaching of metals from cathode materials is an endothermic reaction and thermodynamically favored by high temperature. A high temperature also favours the dissociation of acids and hydrolysis of sucrose present in the molasses (Klasson et al., 2022). As shown in Fig. 4, the percentage of all the metals leached were impaired as the temperature reduced from 90 °C to 30 °C, which supports our choice of 90 °C used in the optimization process. The transition metals (Co, Mn and Ni), with only ~50% leached out at 60 °C, showed a stronger dependence on temperature than lithium. This may be attributed to better hydrolysis at higher temperatures of sucrose in the molasses that reduces the transition metal oxides in the cathode material.

3.5. Chemistry of reductive leaching in molasses-methanesulfonic acid media

Molasses, owing to the presence of sugars (glucose, fructose and sucrose), can function as an eco-friendly reducing agent. It is also known to contain phytochemicals (e.g., flavonoids and phenolics) that have been found to function as reductants (Ali et al., 2019; Pant and Dolker, 2017; Zhang et al., 2018). However, the sugars, because of their stronger reductive ability and higher concentration are the dominant reductant. As shown in Table S2, sucrose is the main carbohydrate in the molasses used in this work. It is a disaccharide and a non-reducing sugar. However, it is easily hydrolyzed in an acidic environment to glucose and fructose, which are single and reducing sugars (Ali et al., 2019; Okonkwo et al., 2021) that can reduce transition metal oxides while, being oxidized to shorter chained organics such as gluconic acid, formic acid, glucaric acid, hydroxymethylfurfurals (HMF) among others (Baral et al., 2015; Pagnanelli et al., 2014). The formed organics also have reductive abilities and hence can be further oxidized (Fu et al., 2019a; Urbańska, 2020). This suggests that, with the oxidation of molasses, the oxides of the transition metal present in the spent cathode material are reduced by the successive oxidation of the sucrose hydrolyzation products and their subsequent oxidation products.

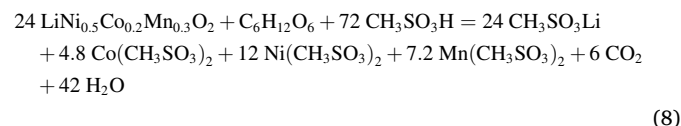
The FT-IR spectra of molasses and the leachates (see Fig. 5) confirm the oxidative degradation of molasses by the cathode materials and the formation of oxidation products during the leaching reaction. The troughs at the region of 3000 and 3650 cm^{-1} , due to the stretching of the -OH group, and peak at 1636 cm^{-1} due to strong hydrogen bonding by formed carboxylic acids are visible and different in the spectra of both molasses and leachates (Fig. 5, Table 1). The shoulder peaks around 2925 and 2878 cm^{-1} due to stretching vibration of the C-H groups of sugars in molasses (El Darra et al., 2017) is absent in the spectra of the leachates while peaks in the fingerprint region (1500–750 cm^{-1}) – the region mostly used for spectra analysis of carbohydrates (Cengiz and Durak, 2019; Kozłowicz et al., 2020) are altered. Prominent characteristic bands such as 923 cm^{-1} in the anomeric region (950–750 cm^{-1}) in molasses, which are typical of stretching and bending vibrations of carbohydrates, are absent in the spectra of the leachates (Cengiz and Durak, 2019; Kozłowicz et al., 2020; Wang et al., 2010). These results suggest that reaction between molasses and cathode materials yields carboxylic acids and other shorter chained organic compounds as shown in Fig. S5.

The FT-IR spectra in Fig. 5 also confirms the formation of metal methanesulfonates salts. As shown in Table 1, peaks due to the symmetric, asymmetric and stretching of functional groups such as SO_3 , C-S, and CH_3 in the formed metal methanesulfonate salts are only apparent in the spectra of the leachates.

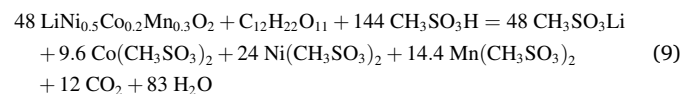
Based on the FT-IR results, the leaching of cobalt, manganese and nickel present in spent cathode materials using molasses-methane

sulfonic acid system may be represented by the chemical reactions shown in Fig. 6 and more generally by eqns. 8 and 9.

Glucose/Fructose as reductant



Sucrose as reductant



4. Conclusion

An environmentally friendly approach for the recovery of the valuable metals from the spent LIBs using sugarcane molasses-methanesulfonic acid media has been explored, and leaching parameters optimized using RSM. The leaching of lithium was found to be strongly dependent on acid concentration and S/L ratio whereas cobalt, manganese and nickel were influenced by the three optimized variables, namely, dosage of molasses, acid concentration and S/L ratio.

Statistical analysis showed that the relationship between methanesulfonic acid concentration, reductant dosage and S/L ratio can be represented by a reduced cubic model. Herein, significant two-way interactions exist between acid concentration and S/L, unlike acid concentration and dosage of the reductant.

Consistent with the predictions from the developed model, complete dissolution of all the metals can be achieved using an acid concentration of 2 M, reductant dosage of 0.408 g/g, S/L ratio of 50 g/L, temperature of 90 °C and time of 2 h. However, further examination of the influence of time showed that the leaching rate of all the metals is fast, with >50% of all the metals leached out within 15 min and nearly complete dissolution (99.9% Li, 99.6% Co, 98.5% Ni and 99.1% Mn) achieved in 60 min. Hence, a leaching time of 60 min was adopted as the new optimal time. Similarly, temperature is proved to have a strong influence on the leaching of all the metals, confirming 90 °C to be the optimal. This is likely due to the enhanced hydrolysis of sugars present in the molasses, and the consequently improved reduction of transition metals, at a high temperature.

In conclusion, the proposed system represents an efficient and eco-friendly approach that utilizes a sustainable agro-industrial by-product (sugarcane molasses) in solving the prevalent challenge of recovering valuable metals present in spent LIBs.

CRedit authorship contribution statement

Emenike G. Okonkwo: Conceptualization, Investigation, Formal analysis, Software, Data curation, Writing – original draft. **Greg Wheatley:** Supervision, Data curation, Writing – review & editing. **Yang Liu:** Supervision, Writing – review & editing. **Yinghe He:** Supervision, Project administration, Resources, Validation, Writing – review & editing.

Declaration of Competing Interest

The authors declare that they have no known competing financial interests or personal relationships that could have appeared to influence the work reported in this paper.

Acknowledgement

The authors wish to acknowledge James Cook University for the postgraduate research scholarship, Wilmar Sugar, Australia for providing the molasses and BatteryWorld, Townsville for the spent lithium-ion batteries.

Appendix A. Supplementary data

Supplementary data to this article can be found online at <https://doi.org/10.1016/j.hydromet.2023.106168>.

References

- Ahn, J., Wu, J., Lee, J., 2019. Investigation on chalcocopyrite leaching with methanesulfonic acid (MSA) and hydrogen peroxide. *Hydrometallurgy* 187, 54–62. <https://doi.org/10.1016/j.hydromet.2019.05.001>.
- Ali, S.E., El Gedaily, R.A., Mocan, A., Farag, M.A., El-Seedi, H.R., 2019. Profiling metabolites and biological activities of sugarcane (*saccharum officinarum* linn.) juice and its product molasses via a multiplex metabolomics approach. *Molecules* 24, 1–21. <https://doi.org/10.3390/molecules24050934>.
- Anjos, O., Campos, M.G., Ruiz, P.C., Antunes, P., 2015. Application of FTIR-ATR spectroscopy to the quantification of sugar in honey. *Food Chem.* 169, 218–223. <https://doi.org/10.1016/j.foodchem.2014.07.138>.
- Bahaloo-Horeh, N., Mousavi, S.M., 2017. Enhanced recovery of valuable metals from spent lithium-ion batteries through optimization of organic acids produced by *aspergillus niger*. *Waste Manag.* 60, 666–679. <https://doi.org/10.1016/j.wasman.2016.10.034>.
- Baral, A.B., Dash, B., Ghosh, M.K., Subbaiah, T., Minakshi, M., 2015. Pathway of sucrose oxidation in manganese (Pyrolusite) nodules. *Ind. Eng. Chem. Res.* 54, 12233–12241. <https://doi.org/10.1021/acs.iecr.5b02881>.
- Cengiz, M.F., Durak, M.Z., 2019. Rapid detection of sucrose adulteration in honey using Fourier transform infrared spectroscopy. *Spectrosc. Lett.* 52, 267–273. <https://doi.org/10.1080/00387010.2019.1615957>.
- Chen, X., Guo, C., Ma, H., Li, J., Zhou, T., Cao, L., Kang, D., 2018. Organic reductants based leaching: a sustainable process for the recovery of valuable metals from spent lithium ion batteries. *Waste Manag.* 75, 459–468. <https://doi.org/10.1016/j.wasman.2018.01.021>.
- Cheng, Q., Chirdon, W.M., Lin, M., Mishra, K., Zhou, X., 2019. Characterization, modeling, and optimization of a single-step process for leaching metallic ions from LiNi 1/3 Co 1/3 Mn 1/3 O 2 cathodes for the recycling of spent lithium-ion batteries. *Hydrometallurgy* 185, 1–11. <https://doi.org/10.1016/j.hydromet.2019.01.003>.
- Church, C., Wuennenberg, L., 2019. Sustainability and second life: the case for cobalt and lithium recycling. *Int. Inst. Sustain. Dev.* 1–68.
- El Darra, N., Rajha, H.N., Saleh, F., Al-Oweini, R., Maroun, R.G., Louka, N., 2017. Food fraud detection in commercial pomegranate molasses syrups by UV–VIS spectroscopy, ATR-FTIR spectroscopy and HPLC methods. *Food Control* 78, 132–137. <https://doi.org/10.1016/j.foodcont.2017.02.043>.
- Fan, E., Yang, J., Huang, Y., Lin, J., Arshad, F., Wu, F., Li, L., Chen, R., 2020. Leaching mechanisms of recycling valuable metals from spent Lithium-ion batteries by a malonic acid-based leaching system. *ACS Appl. Energy Mater.* 3, 8532–8542. <https://doi.org/10.1021/acsaem.0c01166>.
- Fan, X., Tan, C., Li, Yu, Chen, Z., Li, Yahao, Huang, Y., Pan, Q., Zheng, F., Wang, H., Li, Q., 2021. A green, efficient, closed-loop direct regeneration technology for reconstructing of the LiNi0.5Co0.2Mn0.3O2 cathode material from spent lithium-ion batteries. *J. Hazard. Mater.* 410 <https://doi.org/10.1016/j.jhazmat.2020.124610>.
- Faraji, F., Alizadeh, A., Rashchi, F., Mostoufi, N., 2020. Kinetics of leaching: a review. *Rev. Chem. Eng.* 38, 113–148. <https://doi.org/10.1515/revce-2019-0073>.
- Fu, Y., He, Y., Chen, H., Ye, C., Lu, Q., Li, R., Xie, W., Wang, J., 2019a. Effective leaching and extraction of valuable metals from electrode material of spent lithium-ion batteries using mixed organic acids leachant. *J. Ind. Eng. Chem.* 79, 154–162. <https://doi.org/10.1016/j.jiec.2019.06.023>.
- Fu, Y., He, Y., Qu, L., Feng, Y., Li, J., Liu, J., Zhang, G., Xie, W., 2019b. Enhancement in leaching process of lithium and cobalt from spent lithium-ion batteries using benzenesulfonic acid system. *Waste Manag.* 88, 191–199. <https://doi.org/10.1016/j.wasman.2019.03.044>.
- Gao, W., Song, J., Cao, H., Lin, X., Zhang, X., Zheng, X., Zhang, Y., Sun, Z., 2018. Selective recovery of valuable metals from spent lithium-ion batteries – process development and kinetics evaluation. *J. Clean. Prod.* 178, 833–845. <https://doi.org/10.1016/j.jclepro.2018.01.040>.
- Gernon, M.D., Wu, M., Buszta, T., Janney, P., 1999. Environmental benefits of methanesulfonic acid: comparative properties and advantages. *Green Chem.* 1, 127–140. <https://doi.org/10.1039/a900157c>.
- IEA, 2021. *The Role of Critical Minerals in Clean Energy Transitions*. IEA Publ, pp. 1–283.
- International Energy Agency, 2020. *Innovation in batteries and electricity storage* 98.
- Klasson, K.T., Sturm, M.P., Cole, M.R., 2022. Acid hydrolysis of sucrose in sweet sorghum syrup followed by succinic acid production using a genetically engineered *Escherichia coli*. *Biocatal. Agric. Biotechnol.* 39, 102231 <https://doi.org/10.1016/j.bcab.2021.102231>.
- Kozłowicz, K., Różyło, R., Gładyszewska, B., Matwijczuk, A., Gładyszewski, G., Chocyk, D., Samborska, K., Piekut, J., Smolewska, M., 2020. Identification of sugars and phenolic compounds in honey powders with the use of GC–MS, FTIR spectroscopy, and X-ray diffraction. *Sci. Rep.* 10, 1–10. <https://doi.org/10.1038/s41598-020-73306-7>.
- Ku, H., Jung, Y., Jo, M., Park, S., Kim, S., Yang, D., Rhee, K., An, E.M., Sohn, J., Kwon, K., 2016. Recycling of spent lithium-ion battery cathode materials by ammoniacal leaching. *J. Hazard. Mater.* 313, 138–146. <https://doi.org/10.1016/j.jhazmat.2016.03.062>.
- Li, L., Dunn, J.B., Zhang, X.X., Gaines, L., Chen, R.J., Wu, F., Amine, K., 2013. Recovery of metals from spent lithium-ion batteries with organic acids as leaching reagents and environmental assessment. *J. Power Sources* 233, 180–189. <https://doi.org/10.1016/j.jpowsour.2012.12.089>.
- Li, L., Fan, E., Guan, Y., Zhang, X., Xue, Q., Wei, L., Wu, F., Chen, R., 2017. Sustainable recovery of cathode materials from spent Lithium-ion batteries using lactic acid leaching system. *ACS Sustain. Chem. Eng.* 5, 5224–5233. <https://doi.org/10.1021/acssuschemeng.7b00571>.
- Li, P., Luo, S.H., Su, F., Zhang, L., Yan, S., Lei, X., Mu, W., Wang, Q., Zhang, Y., Liu, X., Hou, P., 2022. Optimization of synergistic leaching of valuable metals from spent lithium-ion batteries by the sulfuric acid-malonic acid system using response surface methodology. *ACS Appl. Mater. Interfaces* 14, 11359–11374. <https://doi.org/10.1021/acsaami.1c23258>.
- Ma, Y., Zhou, X., Tang, J., Liu, X., Gan, H., Yang, J., 2021. Reaction mechanism of antibiotic bacteria residues as a green reductant for highly efficient recycling of spent lithium-ion batteries. *J. Hazard. Mater.* 417, 126032 <https://doi.org/10.1016/j.jhazmat.2021.126032>.
- Marçq, O., Barbe, J.M., Trichet, A., Guillard, R., 2009. Reaction pathways of glucose oxidation by ozone under acidic conditions. *Carbohydr. Res.* 344, 1303–1310. <https://doi.org/10.1016/j.carres.2009.05.012>.
- Meng, F., Liu, Q., Kim, R., Wang, J., Liu, G., Ghahreman, A., 2020. Selective recovery of valuable metals from industrial waste lithium-ion batteries using citric acid under reductive conditions: leaching optimization and kinetic analysis. *Hydrometallurgy* 191, 105160. <https://doi.org/10.1016/j.hydromet.2019.105160>.
- Miao, Y., Liu, L., Zhang, Y., Tan, Q., Li, J., 2022. An overview of global power lithium-ion batteries and associated critical metal recycling. *J. Hazard. Mater.* 425, 127900 <https://doi.org/10.1016/j.jhazmat.2021.127900>.
- Montgomery, D.C., 2017. *Design and Analysis of Experiments*, 9th Editio. ed. John Wiley & Sons.
- Okonkwo, E.G., Wheatley, G., He, Y., 2021. The role of organic compounds in the recovery of valuable metals from primary and secondary sources: a mini-review. *Resour. Conserv. Recycl.* 174, 105813 <https://doi.org/10.1016/j.resconrec.2021.105813>.
- Pagnanelli, F., Moscardini, E., Granata, G., Cerbelli, S., Agosta, L., Fieramosca, A., Toro, L., 2014. Acid reducing leaching of cathodic powder from spent lithium ion batteries: glucose oxidative pathways and particle area evolution. *J. Ind. Eng. Chem.* 20, 3201–3207. <https://doi.org/10.1016/j.jiec.2013.11.066>.
- Pant, D., Dolker, T., 2017. Green and facile method for the recovery of spent Lithium nickel manganese cobalt oxide (NMC) based lithium ion batteries. *Waste Manag.* 60, 689–695. <https://doi.org/10.1016/j.wasman.2016.09.039>.
- Parker, S.F., Zhong, L., 2018. Vibrational spectroscopy of methyl methanesulfonates: M = Na, Cs, Cu, Ag, Cd. *R. Soc. Open Sci.* 5, 1–10. <https://doi.org/10.1098/rsos.171574>.
- Peeters, N., Binmemens, K., Riaño, S., 2020. Solvometallurgical recovery of cobalt from lithium-ion battery cathode materials using deep-eutectic solvents. *Green Chem.* 22, 4210–4221. <https://doi.org/10.1039/d0gc00940g>.
- Roshanfar, M., Golmohammadzadeh, R., Rashchi, F., 2019. An environmentally friendly method for recovery of lithium and cobalt from spent lithium-ion batteries using gluconic and lactic acids. *J. Environ. Chem. Eng.* 7, 102794 <https://doi.org/10.1016/j.jece.2018.11.039>.
- Urbanika, W., 2020. Recovery of Co, Li, and Ni from spent li-ion batteries by the inorganic and/or organic reducer assisted leaching method. *Minerals* 10, 1–13. <https://doi.org/10.3390/min10060555>.
- Urias, P.M., dos Reis Meneses, L.H., Cardoso, V.L., de Resende, M.M., de Souza Ferreira, J., 2020. Leaching with mixed organic acids and sulfuric acid to recover cobalt and lithium from lithium ion batteries. *Environ. Technol. (U.K.)* 0, 1–11. <https://doi.org/10.1080/09593330.2020.1772372>.
- Vieceli, N., Nogueira, C.A., Guimarães, C., Pereira, M.F.C., Durão, F.O., Margarido, F., 2018. Hydrometallurgical recycling of lithium-ion batteries by reductive leaching with sodium metabisulphite. *Waste Manag.* 71, 350–361. <https://doi.org/10.1016/j.wasman.2017.09.032>.
- Wang, J., Kliks, M.M., Jun, S., Jackson, M., Li, Q.X., 2010. Rapid analysis of glucose, fructose, sucrose, and maltose in honeys from different geographic regions using Fourier transform infrared spectroscopy and multivariate analysis. *J. Food Sci.* 75, 208–214. <https://doi.org/10.1111/j.1750-3841.2009.01504.x>.
- Wang, Y., Wang, T.-Y., Wu, L.-J., Min, X.-B., Liu, H., Wen, D.-Q., Ke, Y., Wang, Z.-B., Tang, Y.-W., Fu, H.-K., 2019a. Recovery of valuable metals from spent ternary Li-ion batteries: dissolution with amidosulfonic acid and D-glucose. *Hydrometallurgy* 190. <https://doi.org/10.1016/j.hydromet.2019.105162>.

- Wang, B., Lin, X.Y., Tang, Y., Wang, Q., Leung, M.K.H., Lu, X.Y., 2019b. Recycling LiCoO₂ with methanesulfonic acid for regeneration of lithium-ion battery electrode materials. *J. Power Sources* 436, 226828. <https://doi.org/10.1016/j.jpowsour.2019.226828>.
- Wu, Z., Soh, T., Chan, J.J., Meng, S., Meyer, D., Srinivasan, M., Tay, C.Y., 2020. Repurposing of fruit peel waste as a green reductant for recycling of spent lithium-ion batteries. *Environ. Sci. Technol.* 54, 9681–9692. <https://doi.org/10.1021/acs.est.0c02873>.
- Yan, S., Sun, C., Zhou, T., Gao, R., Xie, H., 2021. Ultrasonic-assisted leaching of valuable metals from spent lithium-ion batteries using organic additives. *Sep. Purif. Technol.* 257, 117930 <https://doi.org/10.1016/j.seppur.2020.117930>.
- Yang, J., Jiang, L., Liu, F., Jia, M., Lai, Y., 2020. Reductive acid leaching of valuable metals from spent lithium-ion batteries using hydrazine sulfate as reductant. *Trans. Nonferrous Metals Soc. China* 30, 2256–2264. [https://doi.org/10.1016/S1003-6326\(20\)65376-6](https://doi.org/10.1016/S1003-6326(20)65376-6).
- Yang, Y., Okonkwo, E.G., Huang, G., Xu, S., Sun, W., He, Y., 2021. On the sustainability of lithium ion battery industry – a review and perspective. *Energy Storage Mater.* 36, 186–212. <https://doi.org/10.1016/j.ensm.2020.12.019>.
- Zhang, Y., Meng, Q., Dong, P., Duan, J., Lin, Y., 2018. Use of grape seed as reductant for leaching of cobalt from spent lithium-ion batteries. *J. Ind. Eng. Chem.* 66, 86–93. <https://doi.org/10.1016/j.jiec.2018.05.004>.
- Zhao, Y., Pohl, O., Bhatt, A.I., Collis, G.E., Mahon, P.J., R  ther, T., Hollenkamp, A.F., 2021. A review on battery market trends, second-life reuse, and recycling. *Sustain. Chem.* 2, 167–205. <https://doi.org/10.3390/suschem2010011>.
- Zheng, H., Huang, J., Dong, T., Sha, Y., Zhang, H., Gao, J., Zhang, S., 2022. A novel strategy of lithium recycling from spent lithium-ion batteries using imidazolium ionic liquid. *Chin. J. Chem. Eng.* 41, 246–251. <https://doi.org/10.1016/j.cjche.2021.09.020>.
- Zhong, L., Parker, S.F., 2018. Structure and vibrational spectroscopy of methanesulfonic acid. *R. Soc. Open Sci.* 5, 1–9. <https://doi.org/10.1098/rsos.181363>.